WETTABILITY BY WATER CONTACT ANGLE UPON THE SURFACE OF WOOL FABRICS COVERED WITH OXIDE NANOPARTICLES

M. BIRZU[a,b], L. FRUNZA[a*], I. ZGURA[a], V. F. COTOROBAI[a], C. P. GANEA[a], N. PREDA[a], M. ENCULESCU[a]
[a]*National Institute of Materials Physics, PO Box Mg 07, 077125 Magurele, Romania*
[b]*National Institute of Statistics, 050706 Bucharest, Romania*

Wetting properties of wool textiles were studied either for the raw samples or for those functionalized via covering them at low temperature with nanoparticles of titanium dioxide or zinc oxide. Oxygen plasma pretreatment was performed before deposition. Characterization used optical examination, scanning electron microscopy, infrared spectroscopy, thermogravimetry, X-ray diffraction. Wetting properties were tested under static conditions by estimating the water contact angle. The sessile drop method was applied. The deposited matter represents 3 to 8 wt%, covering rather uniformly the fiber surface. Treated samples show mostly lower values of contact angle than the pristine ones. Cassie-Baxter model is discussed in relation to the equilibrium contact angle of the support.

1. Introduction

Wool is known as a natural fiber which is largely used for clothing and home. Among the textile fibers, wool has a complicated structure (see e.g. [1]). Thus, outside of the wool fiber there is a layer of scales called cuticle, the cells of which overlap like tiles on a roof. The scales have waxy coating which stops water penetration [2,3], wool being water-repellent in the original form. The inner filaments are surrounded by a matrix of high sulfur proteins, making wool absorbent (for water and dyes).

Especially for summer clothing, the (wool) fabrics must be hydrophilic. Plasma [4, 5] or enzyme [6, 7] treatments may improve and stabilize the wool hydrophilic properties [8]. Titanium oxide (TiO_2) or zinc oxide (ZnO) nanoparticles have been successfully attached to different hydrophobic textiles [9-12] including wool [13-17] in order to achieve (more or less) superhydrophilic properties.

The study of the wetting behavior of the wool and of the (single) keratin fibers especially by estimating the contact angles (CAs) was developed for decades [18-28]. Dynamic or static measurements as well as a technique based on the Wilhelmy balance principle [29] were applied in this aim. Moreover, the wetting was used as a measure of the superficial modifications [29] undergone under the (pre)treatments mainly with plasmas.

In this work, wetting properties of knitted Merinos and indigenous (Ţigaie) wool samples were investigated either in the raw form or after the applied treatments: The samples were pretreated by oxygen plasma and then functionalized by deposition of TiO_2 or ZnO nanoparticles at low temperature using procedures already applied in the lab for other textiles. Contact angle values were obtained by sessile drop method. Cassie-Baxter model [30, 31] considered to be functional for heterogeneous surfaces [32], was also discussed for the behavior of our samples. It was found that the wettability was changed according to the new heterogeneity properties and additional roughness introduced by functionalization.

---

*Corresponding author: lfrunza@infim.ro

2. Experimental

2.1. Samples

Wool samples with plain woven structure were either commercial Merino tests kindly provided by Lanerossi (Italy) or by Romanian home/industrial sources. Specific details of the investigated samples are shown in Table 1; some samples are already mentioned in other work [33] for photocatalytic properties. Commercial Merino wools are specifically treated to improve shrink and machine washing resistance by oxidative processes, by covering with specific polymers or by combination of these treatments [34].

Table 1. Wool samples and their characteristics

Sample	Type of textile	Element /yarn	Composition*	Color	Fabrication treatment
LM2	Knitted wear	Nm 2/30	Extrafine Merino	red	Shrink resistant
LM3	Knitted wear	Nm 2/30	Extrafine Merino	red	Total easy care
LM4	Knitted wear	Nm 2/30	Fine Merino	ivory	Shrink resistant
LM20	Knitted wear	Nm 1/15	Extrafine Geelong	beige	
LM21	Knitted wear	Nm 2/15	Extrafine Geelong	beige	
LM23	Knitted wear	Nm 12/30	Extrafine Merino	ivory	
LVsM	Manually knitted glat	Carded yarn, Nm 5	Romanian	brown	Detergent washed; dried in air
LBv	Twill fabric	Nm 10, 720 g/m^2	Romanian	navy blue	Detergent washed; dried in air
LBhS	Satin fabric	Carded yarn, Nm 19, 670 g/m^2	Romanian	kaki	Detergent washed; dried in air
LBhP	Woven fabric	Carded yarn, Nm 17, 690 g/m^2	Romanian	red	Detergent washed; dried in air
L1***	Knitted wear	Nm 2/48	Extrafine Merino	ivory	Total easy care +Antipilling
L18***	Knitted wear	Nm 2/30	Fine Merino	ivory	Total easy care
L19***	Knitted wear	Nm 2/30	Extrafine Merino	ivory	Antipilling
LVs***	Manually knitted glat	Carded yarn, Nm 5	Romanian	blue-green	Detergent washed; dried in air

* Merino (M) materials come from Italy; Vs, Bv, Bh materials come from Romania; ** Nm – metric number is the length density of the yarn (Nm=L/m); *** previously studied for photocatalytic properties [33].

In order to perform changes of the surface, the wollen pieces (of about 1,5x1,5 cm) were firstly washed with n-propylic alcohol and then dried on a dust-free (flat) surface at room temperature.

2.2. Surface functionalization

Surface modification of the textile samples, further called functionalization was carried out using the following methods:

- Oxygen plasma (P) treatment, carried out in the PICO system (Electronic Diener Plasma Technology), at 2-5 minutes at a pressure of 0.3 mbar.

- Covering with TiO$_2$ particles by sol-gel (SG) as detailed in ref. [[35]: The fabrics were dip coated in a TiO$_2$ sol of titanium tetraisopropoxide (Sigma Aldrich).

- ZnO was deposited upon the investigated fabrics by electroless (E) or sputtering (SP) methods as described previously [33, 36, 37]. A Sputter-Coater (Tectra GmbH) installation and a

ZnO target (K.J. Lesker) were used. Deposition time was kept the same in a series of experiments. The incident beam was obtained at 200 W under argon plasma.

Sample notation is as follows: the raw samples keep the material label of Table 1 for the 'substrate' while functionalized samples retain the treatment applied (P, E, SP or SG); for example $TiO_2(SP)/LM21$ means the sample having TiO_2 deposited by sputtering upon LM21 support.

2.3. Characterizing methods

The raw and the coated fabrics were characterized by applying several investigation techniques: X-ray diffraction (XRD) used D8 Advance equipment (Bruker-AXS) with CuK_α radiation. Scanning Electron Microscopy (SEM) used a Zeiss Evo 50 XVP instrument after conventional gold metallization of the samples. Thermogravimetric measurements (TG) were performed with a Diamond TG-DTA apparatus (Perkin Elmer) up to 1050 K, at a heating rate of 10 $Kmin^{-1}$. Loading of the textiles with semiconductor oxide was estimated according to the procedure described previously [38] for other organic-inorganic materials. The layer-substrate interaction was signaled in the derivative DTG and heat flow (HF) curves. Fourier Transform Infrared Spectroscopy (FTIR) was applied in attenuated total reflection (ATR) mode with a Spectrum BX II (Perkin Elmer) instrument by collecting at least 28 scans at 4 cm^{-1} resolution. Direct visualization was also applied through an optical microscope Zeiss with Nikon Coolpix 2000 video camera or Panasonic DMC-FZ8 photo camera. Illumination of the sample fabric was from a fluorescent tube through a translucent diffusing screen [39].

2.4. Wetting properties

The water repellency was evaluated by measuring static contact angles at room temperature with Drop Shape Analyzer DSA 100 (Krüss). The working mode in the case of textile materials has been described elsewhere [41]. A fixed steel needle supplied a water drop of 3 μL onto the surface of the solid sample to be investigated. The image of the sessile drops was captured. The data resulted from processing the images used specific programs to fit the profile with the Young-Laplace or with 2nd degree equations. Finally, one obtains the value of the contact angle (CA). At least five different points on each sample were thus considered.

3. Results and discussion

Complex characterization of investigated textiles (mostly of their surface) was performed leading to structural (physical and some chemical) data before and after functionalization; contact angle values were obtained for water drops upon the samples.

3.1. Structural characterization

Fig. 1 illustrates representative optical images of samples together with a microscope scale which allows a rapid comparison of their "pores" and of geometrical structure. These images are acquired on the optical microscope. The color of the images is not relevant for the real color of the sample. We have a set of samples (L1, LM2, LM3, L18, and L19) which have the same size of the yarn and of the voids, features allowing direct comparing of their wetting behavior.
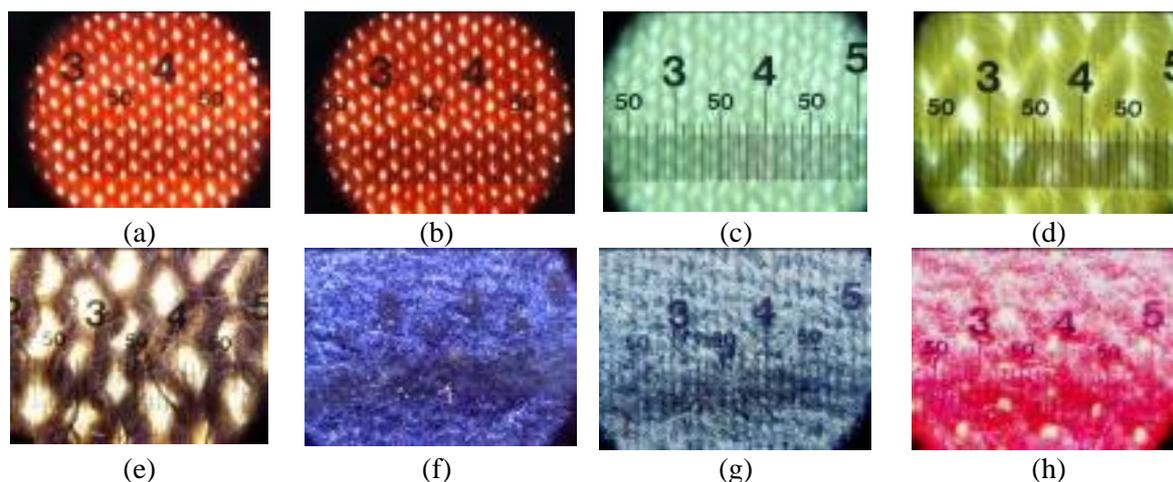
Fig. 1. Optical images of some samples: (a) LM2; (b) L3; (c) LM20;
(d) LM23; (e) LVsM; (f) LBv; (g) LBhS; (h) LBhP. .

Fig. 2 shows the comparison of TG and DTG curves of representative pairs of raw and plasma treated wool samples. In each case one can find (at least) three processes which take place in the wool pyrolysis progress [34, 42]. An initial decrease of ca. 7% is observed from room temperature to 430 K, due to wool dehydration. The second important loss of wool mass (~40 %) occurs from 463 to 623 K. The hydrogen-bonded peptide structure is broken and the ordered regions of the wool undergo a phase change; also a cleavage of the disulphide bonds occurs and volatile matter is released [43]. The temperature onset of decomposition occurs in the order raw wool less than treated wool. This order is expected on the basis of the corresponding pyrrolysis mechanisms. The third process is a mass loss of ca. 45% due to the reaction of char oxidation [44].

We focused by this evaluation on the amount of deposited oxide nanoparticles. Using similar deposition methods, this amount was of the same order of magnitude (3-8 wt%) as upon textiles made from other materials [37].
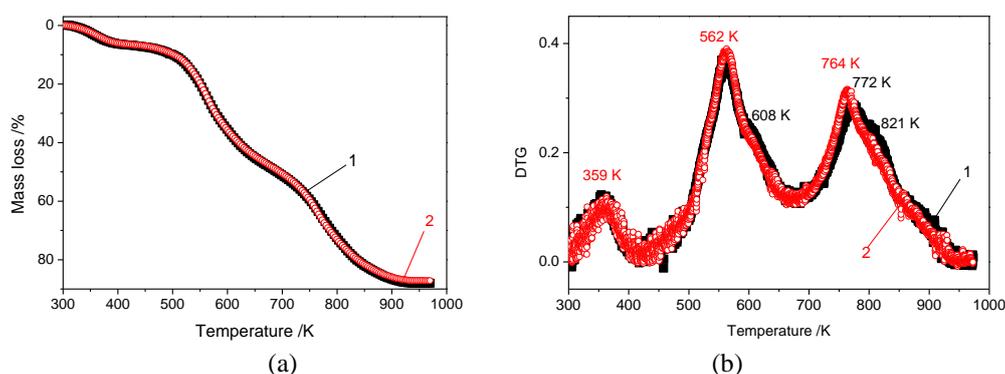

Fig. 2. (a) TG and (b) DTG curves for the samples in raw form or plasma treated
as follows: (1) LM21; (2) LM21P. The temperature at the peaks is shown

In the X-ray diffraction patterns (see some examples in Fig. 3) there are peaks which can be assigned to the ordered part of the wool fibers (usually with biphasic crystalline/amorphous structure) (see e.g. [45]). Two major broad peaks can be observed at *ca.* $2\theta = 9°$ and $23°$ in the pattern of the raw sample which are due to the α-helix and β-sheet structures [46] of the keratin, the main protein component of the wool. The analysis of these patterns demonstrates expected changes [46] due to the ZnO functionalization treatments. Thus, additional sharp XRD reflections at $2\theta = 32.0°$, $34.6°$ and $36.4°$ appear which can be indexed to the reflections (100), (001) and (101) respectively: These peaks confirm the good crystalline nature of the deposited ZnO particles. XRD peaks of the main TiO_2 crystalline forms (anatase, rutile and brookite [47]) cannot be

observed in the patterns obtained for our samples, this fact revealing either the amorphous structure of the coated layers, or the formation of highly dispersed fine particles of oxides (maybe in a too small amount) on these wool supports.
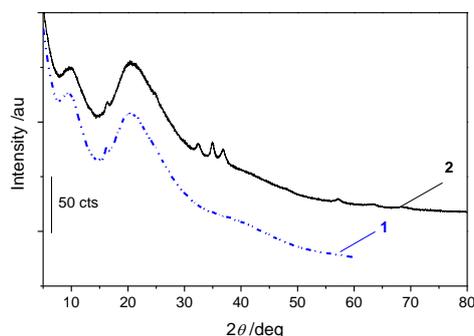

Fig. 3. XRD patterns of LM23 sample (1) in original form and (2) deposited by sputtering with ZnO. The curves were shifted on the ordinate for clarity

The treatments modify also the FTIR spectrum of the substrate, since differences arise in the region of the stretching vibration of -OH, -COOH and amide (-CONH-) groups (vibration at 3300 cm^{-1}) (Figs. 4). The spectrum in the corresponding band of amide was decomposed into Gaussian functions after its transformation in the Kubelka Munk function (Fig. 4). Oxide deposition changes the secondary structure of the wool fibers, leading to slight shifts in the band position and modification of the band shape. Thus, in the case of LM21 sample, the Amide I band has a (rather small) shift from 1637.0 to 1639.4 cm^{-1}. At the same time, the intensity (as band surface) ratio of the amide I band to amide II band $I_{AmideI}/I_{AmideII}$ varies from 0.60 to 1.14. High affinity of titanium dioxide nanoparticles to negatively charged hydroxyl and carboxyl groups has already been proved [48]: Such binding reactions might take place between the titanium dioxide particles and functional groups of the wool. This behavior is similar to that observed for polyamide-ZnO composites [49].
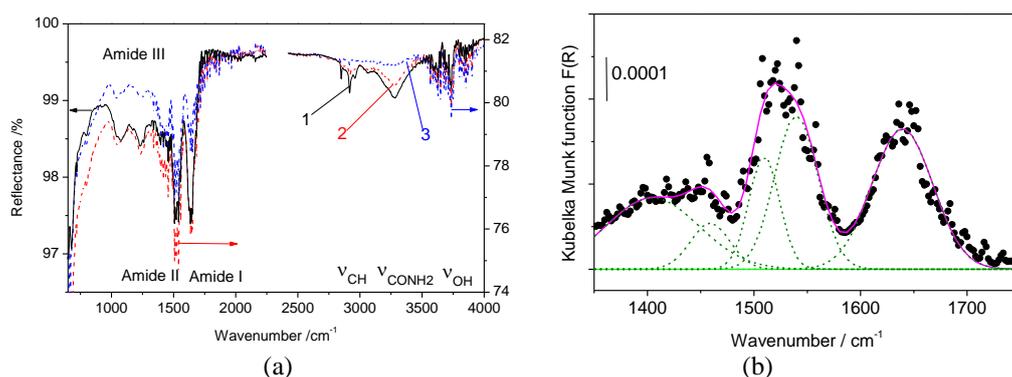

(a)   (b)

Fig. 4. (a) IR spectrum of the LM21 sample, in the raw (1) and treated with TiO$_2$ [(2) and (3)] forms. (b) Decomposition into Gaussians, of the spectrum (1) after its transformation into Kubelka Munk dependence

Fig. 5 presents SEM images of some of the deposited samples. As indicated in the literature, wool external cuticle cells can be observed (Fig. 5a) in a "smooth" surface [42]. Deposited particles are observed on the fiber surface. Aggregation of oxide particles seems to take place randomly on the fiber surface. Sometimes the deposition is though thick and covers the fiber surface. Anyhow, surface roughness of the fabrics significantly increases after oxide coating.
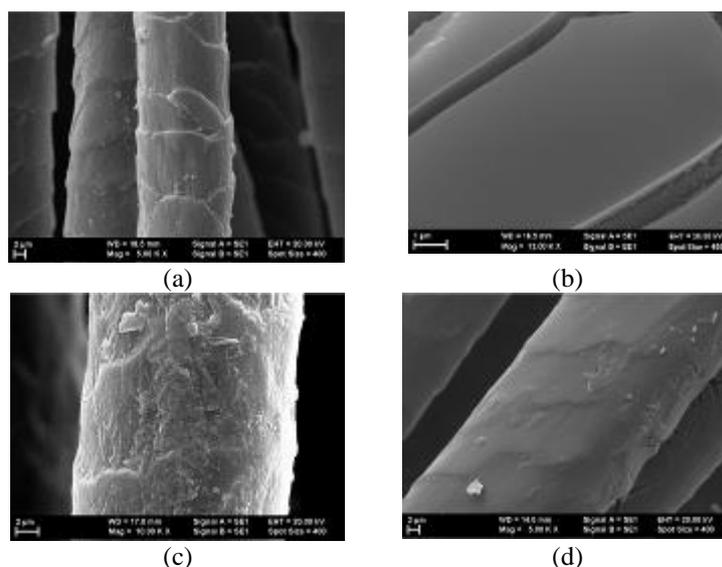
*Fig. 5. SEM images of some deposited samples: (a) ZnO(SP)/LM2;
(b) TiO2(SG)/LM21; (c) ZnO(SP)/LM23; (d) TiO2(SG)/LM23P.*

Hierarchical roughness appears since aggregated oxide nanoparticles sit over the periodic structure of microfiber network (array).

3.2. Wetting properties. Contact angle

The wettability of the materials was measured in terms of the water contact angle. The contact angle of the pristine wool fabric (for example, LM21) was about 155° because of the hydrophobic nature of the keratins (Fig. 6a). After applying the deposition treatment, the water contact angle became 151.2° (Fig. 6b).
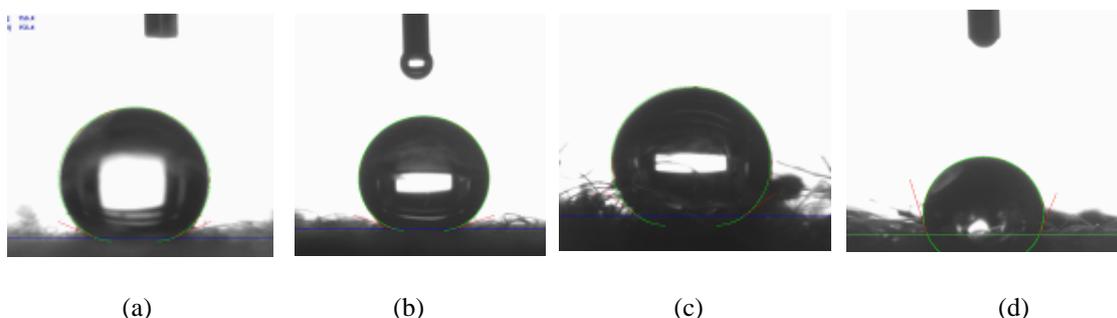

(a) (b) (c) (d)

*Fig. 6. Contact angle evaluated by sessile drop method on different samples:
(a) LM21; (b) TiO2(SG)/LM21; (c) LVsM; (d) ZnO(E)/ LVsM.*

All the samples exhibit hydrophobic properties and even superhydrophobic (water-repelling) ones, the contact angles recording values between 134° and 166°. The importance of the side (front/rear) where the CA measurement is made should be thus highlighted. These measurements were normally taken parally to the privileged direction of the fabric; for the measurements on the perpendicular direction, the values are different.

The growth of ZnO/TiO$_2$ particles takes place on scattered sites, there are nanoparticles inside the voids of the fabric yarns. The fibers are joined in a structure with a micro- and nano-roughness. In addition, fabrics contain capillaries between, and in, the yarns: therefore, the surface of the investigated fabrics is far for being flat, really smooth and homogeneous. The experimentally measured contact angle is in fact an apparent one and can differ considerably from the true (Young) value. The mean CA values of the raw (original) or deposited samples are given in Table 2.

Table 2. Apparent CA values (in degrees) of the investigated samples

Sample	Raw form	Deposited ZnO(E)	Deposited ZnO(SP)	Deposited TiO$_2$(SG)
LVs	141.2	137.9↓	151.6↑	
LVsM	143.9	112.6↓	155.7↑	
LBv	152.3	105.6↓		
LBhS	148.3	155.2↑		
LBhP	<5	130.3↑		
L1	149.3	150.3↑	151.6↑	164.8↑
LM2	166.4		155.7↓	
LM3	133.8	156.0↑		
LM4	147.0	148.7		
L18	152.0	137.5↓	140.7↓	161.5*↑
L19	149.9	145.3↓	165.8↑	147.7*↓
LM20	168.0	164.2↓		150.2*↓
LM21	156.4			161.7
LM22P	138.0			157.2
LM23	136.1		141.2↑	165.1*

* plasma pretreated.

From Table 2 we see that the "raw" materials are hydrophobic, with CA higher than 90°. The samples LM21 and LM23 are also hydrophobic, although they have a rare texture of the fabric. The set of samples mentioned above as having the same size of the yarn and of the voids, have different CA values due to the initial treatment of the yarn/fabric surface (Table 1). CA decreases with a few degrees by the actual surface treatments, the investigated materials become less hydrophobic. The increase in hydrophilicity by plasma treatment could be ascribed to the hydrophilic groups formed on the surface and/or to the fatty-layer elimination as shown for ex. by Canal *et al*. [50].

The complex structure of the investigated fabrics makes difficult the application of known theoretical models to describe their wetting behavior: Our samples being heterogeneous and with (super)hydrophobic porous surfaces, one thought firstly to the Cassie-Baxter equation [30,31] applied in the (usual) form:

$$cos\,\theta_C = f\,cos\,\theta_0 - (1\text{-}f)$$

where θ_C is the contact angle formed on the treated fabric and θ_0 is the contact angle formed on untreated wool fabric. The parameter f (or "roughness factor") is the fraction of the support surface contacting the water droplet; its value can be calculated for each raw-treated pair of samples. The obtained f values are given in Table 3. We looked then for a suitable value of θ_0 for a smooth planar homogeneous layer or at least on fibers of wool or of related materials as hair, keratin etc. Le *at al.* [51] have determined a value for wool fibers by using the liquid droplet method. The value θ_0=76.2° (see Table 3) was obtained using the dynamic contact angles determined by Brooks and Rahman [52] and the formula [53] relating these angles to the equilibrium angle: The f values obtained with this θ_0 are a bit lower and some cases, seem to be better than those corresponding to θ_0=68.4°. We took also into consideration the equilibrium CA determined on the polyamide layers [54], but the f parameters obtained for our samples were even less suitable. There are other experimental determinations in the literature (*e.g.* [20, 21,55, 56]) leading to the water equilibrium angle on wool materials.

Table 3. Parameter f* of the uncoated samples for different θ_0 values

θ_0 ([Ref.]) Sample	68.4 ([51])	76.4 ([52])	50.4 ([54])
LVs	0.01	0.01	0.01
LVsM	1.26	0.99	0.91
LBv	0.74	0.58	0.54
LBhS	0.14	0.11	0.11
LBhP	0.89	0.70	0.64
L1	0.74	0.59	0.54
LM2	0.00	0.003	0.01
LM3	0.50	0.39	0.36
LM4	0.14	0.11	0.10
L18	0.94	0.74	0.68
L19	1.12	0.89	0.81
LM20	0.64	0.51	0.46
LM21	1.23	0.97	0.89
LM22P	1.37	1.08	0.99
LM23	0.32	0.25	0.24

* $f=(1+\cos\theta_C)/(1+\cos\theta_0)$

All the *f* values for uncoated samples are positive in Table 3, meaning that there is only a partial contact of the drop with the top solid surface [57].

The applicability of Cassie-Baxter equation is followed up even less easy for coated samples. Then, the problem of the θ_0 CA was solved by choosing the value $\theta_0=93^{\circ}$ for ZnO deposited samples as it was argued in Ref. [33], of $\theta_0= 35^{\circ}$ for TiO$_2$(SG) deposited samples [58], or of the value of the uncovered support as mentioned in Ref. [59] for ZnO deposited polyester samples, aware that the support (pristine sample) is far for being smooth and homogeneous in the later case. The roughness factor (called parameter) *f* was found to have the values given in Table 4 which are comparable with those found by Ashraf *et al.* [59].

Table 4. Parameter f* of the coated samples for different θ_0 values (in degrees)

θ_0 Sample	ZnO(E) deposited		ZnO(SP) deposited		TiO$_2$(SG) deposited	
	93	θ_C of the support	93	θ_C of the support	35	θ_C of the support
LVs	2.05	132.39	1.78	115.25		
LVsM	1.98	1.03	1.25	0.65		
LBv	1.42	1.26				
LBhS	0.73	3.46				
LBhP	0.97	0.72				
L1	1.98	1.75	1.78	1.57	11.76	1.05
LM2			1.25	218.51		
LM3	1.55	2.04				
LM4	0.52	2.40				
L18	1.84	1.28	0.23	0.16	7.39	0.52
L19	1.80	1.05	0.25	0.14	0.01	0.01
LM20	1.76	1.80			18.97	1.97
LM21					9.43	0.51
LM22P					20.69	1.01
LM23			0.01	0.03	8.66	1.77

Cassie-Baxter equation does not allow to quantify the wettability, however some differences in these properties can be obtained. In fact, there is a whole debate in the literature concerning the applicability of this form of equation. For example, it was already shown [60] that the use of this form of equation might introduce errors in some aspects of wetting such as the prediction and interpretation of contact angle data on surfaces, the effect of liquid penetration into rough surfaces on the contact angle and the stability of the Cassie–Baxter wetting mode. Moreover, Marmur and Bittoun [61] have shown that the equation is approximation which become valid as the drop size becomes sufficiently large compared to the wavelength of the roughness/heterogeneity of the surface. Another form of Cassie-Baxter equation is that discussed by Swain and Lipowsky [62] in relation with the chemically heterogeneous substrates

$$\cos\theta c = \sum_i f_i \cos\theta i$$

where θ_i is the angle taken on a simple planar surface composed entirely of surface component or chemical species i, f_i is the fraction by area of the surface made up of i. But it is a challenge to use these equation forms; besides, these need additional experimental data, obtainable with difficulty.

4. Conclusions

Raw wool samples either of commercial or of Romanian origin were considered. These were functionalized via covering at low temperature with nanoparticles oxides like TiO_2 or ZnO. Before deposition the samples were pretreated in oxygen plasma.

Binding reactions would have occurred between the oxide particles and functional groups of the wool fibers. Oxide deposition might be conducted by the coordination of the transition metal ion to the protein oxygen atoms, this making to slightly shift the position of the vibration (IR) bands and to modify a bit the shape of these bands. Oxide deposition creates thus composite interfaces of hierarchical roughness since aggregated oxide nanoparticles sit over the periodic structure of microfiber array.

Plasma pretreatment and oxide deposition lead to a decreased hydrophobicity of the wool samples, no matter of its origin.

After these treatments, the analyzed samples have modified the wetting properties, due to additional (hierarchical) roughness introduced by oxide deposition and due to the higher heterogeneity on the fiber surface. CA depends on the size of the mesh fabric/knit, on the considered face and on the finishing treatments applied to the constituent fibers. In the case of textile fibers with small diameter, the surface fiber can dominate most of the interactions.

Thus the CA measurements can be used to assess changes in the morphology of the coating, depending on the desired final effect.

References

[1] C.W. Hock, R.C. Ramsay, M. Harris, Textile Res. J. **11**(10), 415. (1941)
[2] A.P.A. Negeri, H.J. Cornell, D.E. Rivett, Textile Res. J. **63**(2), 109 (1993).
[3] M.T. Huson, D.Evans, J. Church, S. Hutchinson, J. Maxwell, G. Corino, J. Struct. Biology, **163**(2), 127 (2008).
[4] C.W. Kan, C.W.M. Yuen, Fibres & Polymers **8**(2), 168 (2007).

930

[5] R. Morent, N. De Geyter, J. Verschuren, K. De Clerck, P. Kiekens, C. Leys, Surf. Coat. Technol. **202**(14), 3427 (2008)

[6] P. Jovancic, D. Jocic, J. Dumic, J. Textile Inst. **89**(2), 390 (1998).

[7] M. Parvinzadeh, S. Moradian, A. Rashidi, M.E. Yazdanshenas, Enzyme Microbiol Technol. **40**(7), 1719 (2007).

[8] D. Chen, L. Tan, H. Liu, J. Hu, Y. Li, F. Tang, Langmuir **26**(7), 4675 (2010).

[9] T. Wang, X.G. Hu, S.J. Dong, Chem. Comm. (18), 1849 (2007).

[10] H.F. Hoefnagels, D. Wu, G. de With, W. Ming, Langmuir, **23**(26), 13158 (2007).

[11] J. Zimmermann, F.A. Reifler, G. Fortunato, L.C. Gerhardt, S. Seeger, Adv. Funct. Mater. **18**(22), 3662 (2008).

[12] M. Montazer, M.M. Amiri, J. Phys. Chem. B. **118**(6), 1453 (2014).

[13] A. Bozzi, T. Yuranova, J. Kiwi, J. Photochem. A: Chemistry. **172**(1), 27 (2005).

[14] S. Wang, W. Hou, L. Wei, H. Jia, X. Liu, B. Xu, Surf. Coat. Technol. **202**(2), 469 (2007).

[15] B. Xu, M. Niu, L. Wei, W. Hou, X. Liu, J. Photochem. Photobiol. A: Chemistry **188**(1), 98 (2007).

[16] M. Montazer, E. Pakdel, Photochem. Photobiol. **86**(2), 255 (2010).

[17] E. Pakdel, W.A. Daoud, X. Wang, Appl. Surf. Sci. **275**(1), 397 (2013).

[18] R. Molina, F. Comelles, M. R. Julia, P. Erra, J. Colloid. Interf. Sci. **237**(1), 40 (2001).

[19] R. Molina, P. Jovancic, F. Comelles, E. Bertran, P. Erra, J. Adhes. Sci. Technol., **16**(11), 1469 (2002).

[20] R. Molina, P. Jovancic, D. Jocic, E. Bertran, P. Erra, Surf. Interface Anal. **35**(2), 128 (2003).

[21] C. Canal, R. Molina, E. Bertran, P. Erra, Fibers & Polymers **9**(4), 444 (2008).

[22] W.S. Tung, W.A. Daoud, Acta Biomater. **5**(1) 50 (2009)

[23] M. Montazer, E. Pakdel, J. Photochem. Photobiol. C – Photochem. Rev. **12**(4), 293 (2011).

[24] B. Tang, J. Wang, S. Xu, T. Afrin, J. Tao, W. Xu, L. Sun, X. Wang, Chem. Eng. J. **185–186**, 366 (2012).

[25] F.A. Sadr, M. Montazer, Ultrason. Sonochem. **21**(), 681 (2014).

[26] S. Mura, G. Greppi, L. Malfatti, B. Lasio, V. Sanna, M.E. Mura, S. Marceddu, A. Lugliè, J. Colloid Interface Sci., **456**(1), 85 (2015).

[27] R. Dastjerdi, M. Montazer, T. Stegmaier, M.B. Moghadam, Colloids Surf. B: Biointerfaces **91**, 280 (2012).

[28] S.R. Saad, N. Mahmed, M.M. Al Bakri Abdullah, A.V. Sandu, IOP Conf. Ser.: Mater. Sci. Engn. **133** (1), 012028 (2016).

[29] Y.K. Kamath, C.J. Dansizer, H.D. Weigmann, J. Appl. Polymer Sci., **22**(8), 2295 (1978).

[30] A.B.D. Cassie, S. Baxter, Trans. Faraday Soc. **40**, 546 (1944).

[31] N. Verplanck, Y. Coffinier, V. Thomy, R. Boukherroub, Nanoscale Res. Lett. **2**, 577 (2007).

[32] M.G. Krishna, M. Vinjanampati, D.D. Purkayastha, Eur. Phys. J. Appl. Phys. **62**(3), 30001 (2013).

[33] L. Frunza, L. Diamandescu, I. Zgura, S. Frunza, C.P. Ganea, C.C. Negrila, M. Enculescu, M. Birzu, Catal. Today In Press, Corrected Proof, Available online 18 March 2017.

[34] J. S. Crighton, W. M. Findon, J. Thermal Analysis, **11**(2), 305 (1977).

[35] I. Zgura, S. Frunza, L. Frunza, M. Enculescu, C. Florica, C.P. Ganea, C.C. Negrila, L. Diamandescu, J. Optoelectr. Adv. Mater. **17**(7-8), 1055 (2015).

[36] N. Preda, M. Enculescu, I. Enculescu, Soft Materials **11**(4), 457 (2013).

[37] L. Frunza, N. Preda, E. Matei, S. Frunza, C.P. Ganea, A.M. Vlaicu, L. Diamandescu, A. Dorogan, J. Polymer Sci. Part B: Polymer Phys. **51**(19), 1427 (2013).

[38] S. Frunza, H. Kosslick, A. Schonhals, L. Frunza, I. Enache, T. Beica, J. Non-Cryst. Solids **325**(1-3), 103 (2003).

[39] I. Zgura, S. Frunza, L. Frunza, M. Enculescu, C. Florica V.F. Cotorobai, C.P. Ganea, Rom. Rep. Phys., **68**(1), 259 (2016).

[40] T. Beica, L. Nistor, C. Morosanu, L. Frunza, G.E. Stan, I. Zgura, D. Marcov, A. Dorogan, E. Carpus, J. Optoelectr. Adv. Mater.**10**(10), 2811 (2008).

[41] A. C. Popescu, L. Duta, G. Dorcioman, I. N. Mihailescu, G. E. Stan, I. Pasuk, I. Zgura, T. Beica, I. Enculescu, A. Ianculescu, I. Dumitrescu, J. Appl. Phys. **110**(6), 064321 (2011)

[42] M. Forouharshad, M. Montazer, M.B. Moghadam, O. Saligheh, Thermochim. Acta **520**(1-2), 134 (2011).

[43] P.J. Davies, A.R. Horrocks, M. Miraftab, Polym. Int. **49**(10), 1125 (2000).

[44] B.L. Symonowicz, S. Sztajnowski, A. Kulak, Infrared Radiation, Chapter II. IR Spectroscopy as a Possible Method of Analysing Fibre Structures and Their Changes Under Various Impacts, Ed. V. Morozhenko, 2012. 27-40.

[45] J. Cao, C.A. Billows, Polym. Int. **48**(10), 1027 (1999).

[46] M. Montazer, A. Behzadnia, M.B. Moghadam, J. Appl. Polym. Sci., **125**(S2), E356 (2012).

[47] A. Bhattacharyya, S. Kawi, M. B. Ray, Catal. Today. **98**(3), 431 (2004).

[48] W.A. Daoud, S.K. Leung, W.S. Tung, J.H. Xin, K. Cheuk, K. Qi, Chem. Mater. **20**(4), 1242 (2008).

[49] M. Hajibeygi, M. Shabanian, M. Omidi-Ghallemohamadi, H.A. Khonakdar, Appl. Surface Sci. **416**, 628 (2017).

[50] C. Canal, R. Molina, P. Erra, A. Ricard, Eur. Phys. J. Appl. Phys. **36**(1), 35 (2006).

[51] C.V. Le, N.G. Ly, M.G. Stevens, Textile Res. J. **66**(6), 389 (1996).

[52] J.H. Brooks, M.S. Rahman, Tecxtile Res. J.**56**(3), 164 (1986).

[53] R. Tadmor, Langmuir.**20**(18), 7659 (2004).

[54] M. Bachurová, J. Wiener, J. Eng. Fibers & Fabrics **7**(4), 22 (2012).

[55]T.J. Horr, Textile Res. J.**67**(1), 1 (1997).

[56] C. W. Extrand, S.I. Moon, Langmuir, **26**(22), 17090 (2010).

[57] H.Y. Erbil, C.E. Cansoy, Langmuir, **25**(25), 14135 (2009).

[58] S.-H. Nam, S.-J. Cho, C.-K. Jung, J.-H. Boo, J. Šícha, D. Heřman, J. Musil, J. Vlček, Thin Solid Films **519**(20), 6944 (2011).

[59] M. Ashraf, C. Campagne, A. Perwuelz, P. Champagne, A. Leriche, C. Courtois, J. Colloid Interface Sci. **394**, 545 (2013)

[60] A.J.B. Milne, A. Amirfazli, Adv. Colloid Interface Sci. **170**(), 48 (2012).

[61] A. Marmur, E. Bittoun, Langmuir, **25**(3), 1277 (2009).

[62] P.S. Swain, R. Lipowsky, Langmuir, **14**(23), 6772 (1998).